Available online at www.sciencedirect.com

SciVerse ScienceDirect

journal homepage: www.elsevier.com/locate/he

The synthesis of Ni-activated carbon nanocomposites via electroless deposition without a surface pretreatment as potential hydrogen storage materials

M.Z. Figueroa-Torres [a,*], C. Domínguez-Ríos [a], J.G. Cabañas-Moreno [b], O. Vega-Becerra [a], A. Aguilar-Elguézabal [a]

[a] Laboratorio de Catálisis, Departamento de Química de Materiales, Centro de Investigación en Materiales Avanzados, S.C. Miguel de Cervantes 120, Complejo Industrial Chihuahua, C.P. 31130 Chihuahua, Chihuahua, Mexico

[b] Departamento de Ciencia de Materiales, ESFM-IPN UP-ALM, Apdo. Postal 21-408, C.P. 04021, D.F., Mexico

ARTICLE INFO

Article history:
Received 24 December 2011
Received in revised form
16 April 2012
Accepted 20 April 2012
Available online 17 May 2012

Keywords:
Ni-nanoparticle
Electroless
Hydrogen storage
Activated carbon
Spillover

ABSTRACT

This work presents the deposition of Ni nanoparticles on a potassium hydroxide (KOH) activated carbon (AC) support by an electroless deposition (ED) technique without using sensitization and activation surface pretreatments. The hydrogen storage properties of Ni-activated carbon nanocomposites (Ni/AC) were investigated at room temperature and under moderate pressure. The chemical composition, morphology and textural parameters are characterized using an inductively coupled plasma spectrometer (ICP), scanning and transmission electron microscopy (SEM and TEM) and N_2 adsorption isotherms. Fine and well-dispersed Ni nanoparticles were obtained by ED that had spherical shape with an average size of 5 nm. The hydrogen storage capacity of the AC can be improved through Ni loading; which results in a hydrogen storage enhancement factor of two compared with the Ni-free AC. This enhancement factor is due to the greater interactions between the Ni and the AC, which facilitate the hydrogen spillover mechanism.

1. Introduction

Easy access to an adequate energy supply determines the course of development in every human activity. With population growth and advancement in living standards, there is an ever increasing demand for energy worldwide. One of the biggest goals of science is to find clean, non-polluting alternatives to fossil fuel energy sources. In many of these alternatives, hydrogen is seen as an ideal energy carrier for future stationary and non-stationary applications due to its highly-efficient and clean production and utilization [1,2].

The actual challenge for using hydrogen as an energy carrier consists in the development of a hydrogen storage system that operates at moderate temperature and pressure, minimizes weight and volume, while maintaining a reasonable cost [3]. Carbonaceous materials offer many advantages when applied as hydrogen storage materials: low density, large surface area, chemical stability and fast adsorption/desorption kinetics [4]. At cryogenic temperatures researchers have demonstrated that AC with a high micropore volume is the most appropriate material for hydrogen adsorption because of the high hydrogen storage capacity when

* Corresponding author.
E-mail addresses: m_zyzlila@yahoo.com.mx, m.zyzlila@gmail.com (M.Z. Figueroa-Torres).

0360-3199/$ – see front matter
doi:10.1016/j.ijhydene.2012.04.097

compared to other carbonaceous materials [4–6]. However, hydrogen storage capacity at room temperature for all carbonaceous materials is low [4,5]. A promising way to increase it has been through surface modifications that load metal nanoparticles (e.g. Pt, Pd, Ni, Ru and Co) onto the surface of the carbon materials to promote the spillover mechanism, which has been experimentally validated by many groups [7–12]. For example, Yang et al. [8,12], Chen et al. [11] and other groups [7,9,10] had reported that the effective dissociation of hydrogen onto a metal particle with subsequent spillover strongly depended on the particle size and the contact between the support surface and the particle. In addition, the spillover mechanism is active only if the majority of the metal nanoparticles are exposed to hydrogen during the adsorption process.

Some of the experimental techniques to prepare metal-carbon nanocomposites are as follows: wet impregnation [7,9,11], plasma reduction [8], sputtering [13], electrodeposition [14,15] and thermal evaporation [16]. Wet impregnation is the most commonly used, but good control of particle size and morphology are lacking. Electrodeposition requires additional electricity and electrodes. Moreover, some of these techniques require sophisticated equipment, long processing times and may induce the destruction of the carbon structure. On the other hand, electroless deposition (ED) with a pretreatment of $SnCl_2$ sensitization followed by $PdCl_2$ activation is an effective route to deposit metal nanoparticles [17–23]. There are several advantages with the ED technique: high reproducibility, low cost; a simple process and the requirement of very simple equipment [17–23]. Nevertheless, the ED process free of surface pretreatments is of particular interest in order to avoid the use of Pd since it is a high cost metal. However, the effect of the Ni particle distribution on the AC surface and their influence on hydrogen storage capacity, when the ED technique is employed without using conventional surface pretreatments, has not been investigated.

In this paper, an ED method without pretreatment (i.e. sensitization and activation) was developed to deposit highly dispersed Ni-nanoparticles on the surface of a KOH chemically AC in one step. Two ED baths with different reducing agents were studied in order to investigate the effect of bath chemistry. The particle shape and distribution of the Ni-nanoparticles on the AC were characterized. The hydrogen adsorption/desorption properties were measured at 303 K over a range of pressures from 0.01 to 5 MPa to study the influence of the metal on the hydrogen sorption property and to understand the influence of the presence of Ni in the hydrogen storage mechanism. The results have been compared with those of Ni-free AC and discussed. This information might be useful for the development of efficient carbon hydrogen storage materials.

2. Experimental

First, AC was synthesized by the chemical activation of *quercus agrifolia* char with KOH. Char bites with particle sizes of 1.68–2.38 mm were physically mixed with the KOH powder in a weight ratio of 4KOH/1Char. The mixture was placed in a stainless steel rotary reactor and heated in a horizontal tube furnace until it reached 1033 K at a heating rate of 5 K/min with a constant nitrogen flow rate of 250 cm^3/min. The activation was performed for 1 h and then cooled to ambient temperature under the same gas flow rate. The AC was washed with distilled water, then suspended in 5 M HCl and finally rinsed with distilled water. The samples were dried at 383 K for 8 h.

The AC was doped with Ni nanoparticles using the ED technique. The electroless bath formulation consisted of dimethylamine-borane (DMAB, $C_2H_{10}BN$) and hydrazine (N_2H_4) as reducing agents which are listed in Table 1. The ED baths were prepared from analytical grade chemicals and distilled water in a beaker and the components were mixed in the order shown in Table 1. The conditions of the electroless treatment with DMAB were taken from the work of Mallory and Hajdu [21] and the work of Haag et al. [23] for hydrazine; in both cases the original treatments were designed for the plating of metallic surfaces. The processes were modified to favor the deposit on the activated carbon substrate.

For the hydrazine-based bath, sodium hydroxide (NaOH) was used to maintain the pH around 9.6. The ED was conducted on a hot plate with a magnetic stirrer at bath temperatures of 323, 333 and 343 K. In this work, sensitization and surface activation pretreatments were unnecessary to initiate nickel deposition; activated carbon was directly immersed in the electroless bath. After electroless treatment, the Ni/AC samples were separated from the solution by filtration, rinsed several times with distilled water and dried at 383 K.

Morphology of the samples was observed on a JEOL JSM-5800LV scanning electron microscope (SEM) and a high-resolution transmission electron microscopy (HRTEM)

Table 1 – Electroless nickel baths formulation.

	Chemical compound	DMAB-based bath	Hydrazine-based bath
Ni precursor (mol/L)	$NiSO_4 \bullet 6H_2O$	0.12	–
	$Ni(C_2H_3O_2)_2 \bullet 4H_2O$	–	0.12
Complexing agent (mol/L)	$Na_3C_6H_5O_7 \bullet 2H_2O$	0.08	–
	$C_{10}H_{14}N_2Na_2O_8 \cdot 2H_2O$	–	0.16
Stabilizing agent (mol/L)	$C_7H_5NS_2$	0.003	–
	$C_3H_6O_3$	–	0.15
Reducing agent (mol/L)	$C_2H_{10}BN$	0.066	–
	N_2H_4		0.40

Philips model CM-200 equipped with energy dispersive spectroscopy (EDS) analysis.

The amount of Ni deposited on the AC was measured with an inductively coupled plasma (ICP) spectrometer. Samples for ICP were prepared by dissolving Ni-AC in a HCl solution with a known volume. The wt. % of the metal loading with respect to AC can be calculated from the measured concentration of the solution.

Textural characterization was carried out by physical N_2 adsorption/desorption isotherms at 77 K using an automatic gas sorption analyzer (Quantachrome Autosorb 1). Prior to the measurements, the samples were degassed at 573 K for 3 h. The surface area (A_{BET}) was obtained using the multipoint BET method [24,25]. Micropore volume (V_{MI}) was calculated from the adsorption isotherms by applying the Dubinin–Radushkevich (DR) equation. Total pore volume (V_T) was determined at 0.995P/P_0 and mesopore volume (V_{ME}) was calculated as the difference between V_T and V_{MI} [24,25].

Hydrogen storage was evaluated at 303 K over a range of pressures from 0.01 to 5 MPa with a gravimetric system that was equipped with a magnetic levitation microbalance PCTM-6000 (Techno System CO, LTD) and a vacuum system. All weight changes for adsorption/desorption data were corrected with a blank calibration to eliminate the buoyancy effect. Before each analysis, samples were degassed *in-situ* at 673 K for 3 h. The sample weight for each analysis was fixed at 1 g. To avoid all traces of condensable vapors that might affect gravimetric measurements ultra-high purity hydrogen was used.

3. Results and discussion

A typical process for the ED of metals on carbonaceous materials surfaces requires a pretreatment called sensitization and activation prior to ED [17–22]. This consists of the immersion of the substrate in a $SnCl_2$ solution with subsequent immersion in a $PdCl_2$ solution leaving metallic Pd atoms that act as seeds for the ED of the metal. In this work, the Sn–Pd pretreatment step was unnecessary to deposit Ni nanoparticles onto the AC surface. The AC surface contains plenty of hydroxyl groups (OH^-) [26], consequently, the success of the ED of nickel nanoparticles is due to the OH^- groups attached to the surface. The OH^- groups act as nucleation sites for subsequent metal deposition, so the deposition process is greatly simplified in time and cost because of Pd is an expensive noble metal.

Fig. 1 illustrates the steps of Ni deposition onto the AC surface. In the first step, nickel ions react with OH^- groups bonded to AC surface, thus forming a nickel hydroxide bonded to the AC surface. This nickel hydroxide is reduced by electrons from the reducing agent, thereby forming a nickel seed for the subsequent formation of nickel nanoparticles. Then, upon the addition of more Ni atoms, the formation of Ni agglomerates are favored; over a long deposition time a uniform Ni film could be formed. The deposition rate increases with the number of Ni-deposited sites and exhibits an autocatalytic behavior [27].

The ED mechanism for both reducing agents (DMAB and hydrazine) should be similar. The process occurs at the solid–liquid interface, it involves reduction–oxidation reactions with electrons transferred through the interface. The DMAB reaction involves the formation of H_3BO_3 with the release of three hydride ions (H^-), which delivers the electron pair to the nickel's ions reduction. Theoretically each DMAB molecule can reduce three nickel ions. The deposit obtained when DMAB is used is a mixture of metallic nickel and a Ni-B alloy [20,21]. The reduction of the Ni^{+2} with DMAB can be described with the following equations [20,21].

$$3Ni^{+2}(CH_3)_2NHBH_3 + 3H_2O \rightarrow 3Ni^0 + (CH_3)_2NH_2^+ + H_3BO_3 + 5H^+ \quad (1)$$

$$2\left[(CH_3)_2NHBH_3\right] + 5Ni^{+2} + 3H_2O \rightarrow Ni_3B + 2Ni^0 + 2\left[(CH_3)_2NH_2^+\right] + H_3BO_3 + 6H^+ + \frac{1}{2}H_2 \quad (2)$$

When hydrazine is used as the reducing agent, a pure metallic nickel is obtained. In this process, hydrazine is oxidized to give N_2 and water with the simultaneous release of electrons [21,23]. The electroless reduction of Ni^{2+} in the solution, when hydrazine is used as reducing agent, can be described with the following equations [21,23]:

$$N_2H_4 + 4OH^- \rightarrow N_2 + 4H_2^0 + 4e^- \quad (3)$$

$$N_2H_5^+ \rightarrow N_2 + 5H^+ + 4e^- \quad (4)$$

The overall reaction can be written as:

$$2Ni^{+2} + N_2H_4 + 4OH^- \rightarrow 2Ni^0 + N_2 + 4H_2O \quad (5)$$

Fig. 2 shows weight percent of Ni as a function of the deposition time and temperature. For the DMAB bath, deposition rate is low during the first 10 min of deposition, the highest deposition rate is observed between 10 and 15 min and

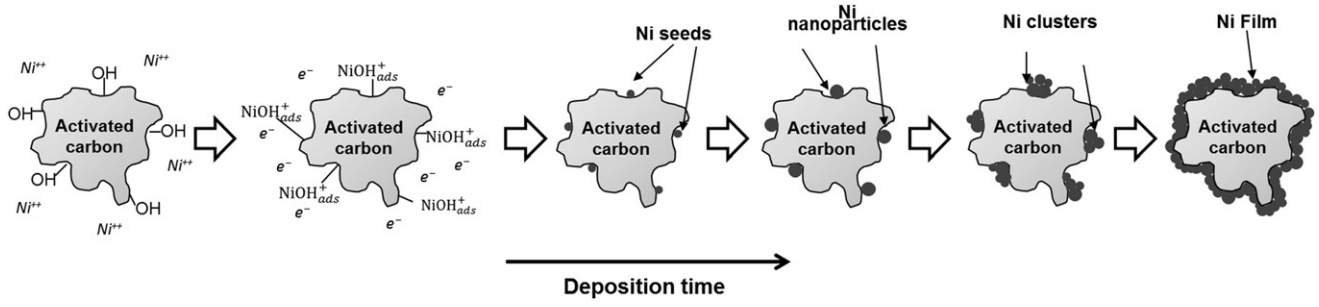

Fig. 1 – Representation of the stages in the electroless deposition of metallic nickel on the activated carbon surface.

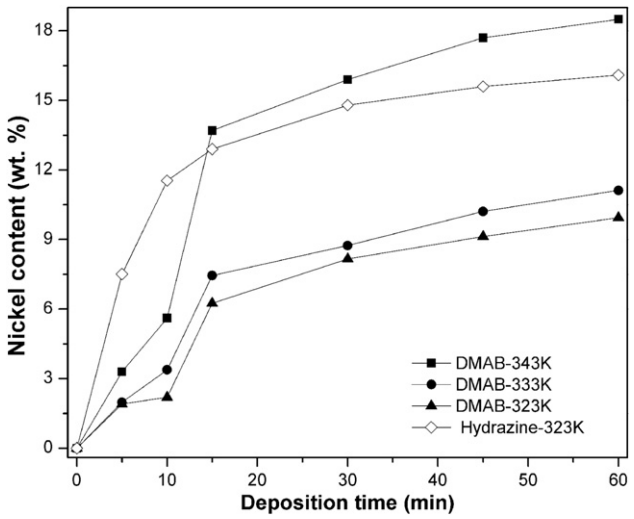

Fig. 2 – Weight percent of Ni as function of deposition time and temperature for DMAB and hydrazine based baths.

then the deposition rate decreases as the time is prolonged to 30 min. At 343 K, the Ni content is so high that the total coating of AC particles was visually detected, the formation of Ni films of approximately 2 μm on the external surface of AC became evident for a Ni content above 17 wt.% (Fig. 3a). The behavior of the ED of Ni at 333 and 323 K were very similar. After 5 min ~ 2 wt. % of Ni was detected; after 1 h, Ni deposition was below 11wt.%, which indicates that the effect of temperature is a more crucial factor governing the quantity of Ni deposited onto the surface than deposition time.

The hydrazine bath shows a better behavior than the DMAB bath because the deposition starts immediately, and the deposition rate seems to be more uniform. Approximately 65% of the total nickel deposited was fixed to surface during the first 10 min of deposition time. Deposition of nickel after 30 min was negligible, and nickel deposited at this time maintained the condition of nanoparticles dispersed over the surface of the activated carbon (Fig. 3c). The drop in the deposition rate, after 30 min, for the hydrazine bath could be primarily caused by the decomposition of the reducing agent followed by a decrease in the number of available Ni^{2+} ions in the bath [27].

Representative TEM micrographs of the Ni/AC deposited using both the DMAB and hydrazine based baths are shown in Fig. 3b and c. In these figures, two phases are clearly observed: one is the amorphous structure, which is characteristic of the AC material where the dark spots are the Ni nanoparticles; the Ni peaks appearing in the EDS spectrum shown in Fig. 3d confirm their presence. Some oxygen was also detected, which is attributed to the OH^- groups of the AC surface. As can be observed in Fig. 3b, Ni nanoparticles obtained using the DMAB bath form Ni-agglomerates. In these Ni-agglomerates, darker small points can be observed; this could be related to the mixture of Ni and Ni-B phases. In contrast, metal

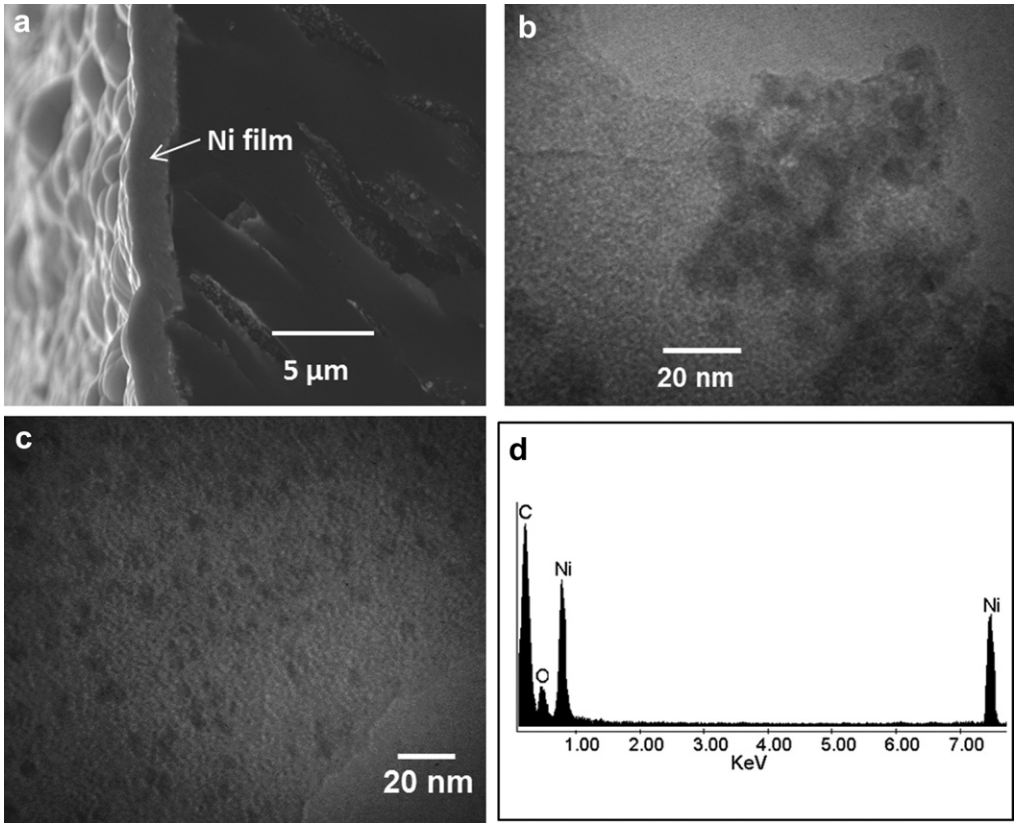

Fig. 3 – Images of Ni-AC nanocomposites, a) and b) samples prepared using a DMAB-based bath at 343 K and 323 K respectively, c) Ni nanoparticles from a hydrazine based bath at 323 K, d) EDS of the region. Deposition time for all samples was 45 min.

nanoparticles deposited with a hydrazine based bath are homogeneously distributed through all carbon surfaces. Ni-nanoparticles present a spherical shape with a particle size from a few nanometers to ~8 nm (Fig. 3c).

Textural parameters, Ni and B amount of some selected samples are listed in Table 2. An analysis of the N_2 adsorption/desorption isotherms obtained from the carbon samples indicated that, according to IUPAC classification, all samples present the typical type I isotherms with a small hysteresis loops (not shown). This indicates a large amount of micropores with little mesoporosity contribution [25].

The Ni-free AC has a A_{BET} of 3089 m^2/g and a total pore volume of 1.697 cm^3/g, which correspond to 84% microporosity. It can be seen that the surface area and the pore volume decrease when Ni is loaded into the AC. The decrease in surface area and pore volume can be attributed to an increased weight and blocking or filling of the pores of the AC by the Ni metal nanoparticles.

Hydrogen adsorption/desorption isotherms for Ni-free AC and Ni/AC nanocomposites at 303 K over the hydrogen pressure range from 0.1 to 5 MPa are shown in Fig. 4. For all samples, a nearly linear relationship exists between hydrogen storage and pressure.

Fig. 4a shows hydrogen adsorption at low pressure from 0.01 to 0.1 MPa, It is observed a little adsorption of hydrogen due mainly to physisorption. The Ni-AC samples absorb more hydrogen because Van der Waals interactions are higher between the Ni nanoparticles and the hydrogen molecules as a first step for the spillover mechanism [8,12,20].

On the other hand, hydrogen storage saturation, at 5 MPa, was not observed; thereby, indicating that a greater hydrogen capacity can be expected at higher pressures. When the pressure is released, hydrogen is desorbed instantaneously in almost the same way as the adsorption, indicative of a reversible behavior. These rates of desorption meet the targets of the USA Department of Energy [28].

Differences can be found in the hydrogen storage capacity of Ni/AC nanocomposites prepared using DMAB and hydrazine based baths with the same Ni content. These differences may be due to the uniformity, size and distribution of the Ni nanoparticles on the AC surface. The Ni/AC nanocomposites from the DMAB-based bath form clusters of Ni and Ni-B nanoparticles, which cause a reduction in the active sites for physical or chemical adsorption; therefore, the hydrogen storage capacity is inferior.

Fig. 5 shows the hydrogen storage capacities at 303 K and 5 MPa for Ni-free AC and the Ni/AC nanocomposites as a function of nickel content and textural characteristics. At 5 MPa Ni-free AC presents a hydrogen storage capacity of 0.82 wt. %; by loading it between 10 and 16 wt.% of Ni nanoparticles, the hydrogen storage capacity can be duplicated. This improvement cannot be attributed to the differences in surface area or porosity because in fact the Ni/AC samples have lower values than Ni-free AC. According to the literature [29], the solubility of hydrogen into Ni nanoparticles is also discarded because of the negligible hydride formation under our experimental conditions. Therefore, this enhancement is attributed to a synergistic effect obtained by the combination of Ni nanoparticles and the AC favoring the spillover kinetics. Ni nanoparticles assist in the dissociation of hydrogen molecules into hydrogen atoms; thereby, allowing the migration of the hydrogen atoms to the AC surface, which then settle down in the pores or on the AC surface. In contrast, Ni-free AC can only physisorb hydrogen molecules via Van der Waals interactions to form only a monolayer promoted by the pressure.

Fig. 5, also shows that hydrogen storage capacity of the Ni/AC nanocomposites depend strongly on the Ni amount. However, it can be observed that for Ni content higher that 10 wt.% the increase in the hydrogen storage is negligible. For Ni contents greater than 16 wt.%, an adverse effect on the hydrogen spillover could be present due to the agglomeration of Ni nanoparticles, possibly covering the AC surface and isolating it from hydrogen exposure, thereby blocking the access to porosity.

The increase in the hydrogen storage capacity due to the dispersion of Ni nanoparticles has been previously reported [9,10,14–22,31–35]. However, the hydrogen storage capacity obtained in this work is superior than many of these studies under similar measurement conditions; some of the reported work used precious metals (e.g palladium, platinum and ruthenium) [7,8,10,12,18,20,22,30–33]. This higher hydrogen storage capacity can be understood from the following aspects. The nanosized Ni particles prepared by ED enable maximum contact with the hydrogen molecules that in combination with the AC surface properties may form a special interface promoting spillover kinetics; the energy

Table 2 – Ni content and textural characterization results.

Electroless bath	Sample	wt. %		A_{BET}[a] (m^2/g)	V_T[b] (cm^3/g)	V_{MI}[c] (cm^3/g)	V_{ME}[d] (cm^3/g)
		Ni	B				
–	AC	–	–	3089	1.697	1.428	0.269
DMAB-based bath	B-6Ni/AC	6.08	0.17	2414	1.343	1.141	0.202
	B-10Ni/AC	9.54	0.33	2086	1.128	0.949	0.179
Hydrazine-based bath	H-6Ni/CA	6.24	–	2465	1.358	1.180	0.178
	H-10Ni/CA	10.67	–	1957	1.090	0.962	0.128
	H-16Ni/CA	16.14	–	1467	0.754	0.646	0.108

a A_{BET}: BET surface area.
b V_T: Total pore volume.
c V_{MI}: Micropore volume.
d V_{ME}: Mesopore volume.

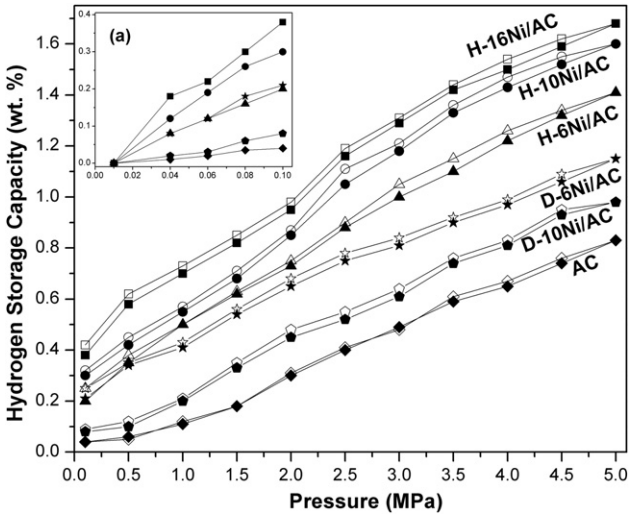

Fig. 4 – High pressure hydrogen adsorption–desorption isotherms at 303 K for Ni-free AC and various Ni/AC samples deposited using DMAB (D) and hydrazine (H) based baths. (Adsorption data are shown as filled symbols, desorption data as open symbols). (a) An Inset of low pressure adsorption.

barrier for transporting the dissociated hydrogen atoms can be minimized [10]. Therefore, the amount of metal loading is not the only factor governing hydrogen storage behavior of a receptor; the importance of particle size, distribution and uniformity are also crucial.

Finally, the elimination of surface pretreatment steps and the quite high hydrogen storage capacity obtained at 5 MPa and room temperature make the ED very promising for metal nanoparticle deposition. To the best or our knowledge, no previous research has been published on ED of Ni/AC without using surface pretreatments. Therefore, by adjusting the ED parameters, improved hydrogen storage performance can be achieved with an optimum Ni loading. Nickel is sufficiently active and less expensive than precious metals while AC is cheap and available at industry levels; thus, economically large-scale production of Ni/AC nanocomposites using ED should be achievable.

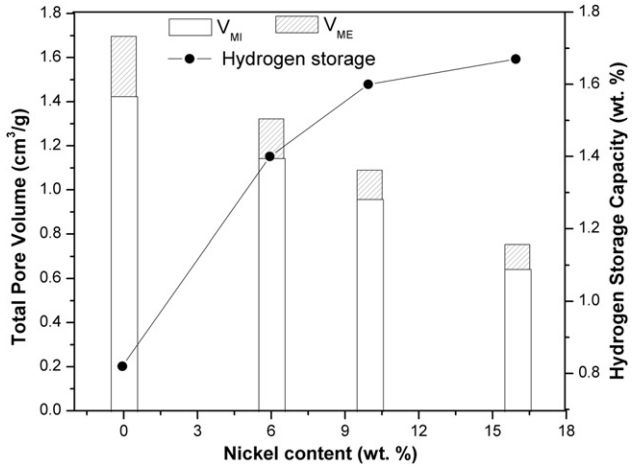

Fig. 5 – Hydrogen storage capacities at 303 K and 5 MPa of AC and Ni/AC nanocomposites obtained from hydrazine based bath as function of nickel content and textural characteristics.

4. Conclusions

Ni/AC nanocomposites could be prepared in one step by ED without requiring surface pretreatments that position ED as a fast, economical and suitable technique to prepare Ni/AC nanocomposites. Well dispersed Ni nanoparticles on the carbon surface were obtained at 323 K using a hydrazine-based bath with a uniform Ni nanoparticle mean size of approximately 5 nm. Results indicated that Ni/AC nanocomposites could be a promising hydrogen storage material, AC provides adequate sites for hydrogen sorption and the presence of Ni nanoparticles improve the hydrogen storage capacity via a spillover mechanism. The hydrogen storage capacity of the H-10Ni/AC nanocomposite was 1.6 wt.%, which was two times higher than the free-Ni AC. Hydrogen storage capacity is strongly dependent on the amount of the Ni deposited, which can be controlled by adjusting ED parameters.

Acknowledgments

The authors would like to thank CONACYT for the financial support of this research though project No. 47776.

REFERENCES

[1] Bakker S. Hydrogen patent portfolios in the automotive industry - the search for promising storage methods. Int J Hydrogen Energy 2010;35:6784–93.
[2] Sahaym U, Grant Norton M. Advances in the application of nanotechnology in enabling a hydrogen economy. J Mater Sci 2008;43:5395–429.
[3] Satyapal S, Petrovic J, Read C, Thomas G, Ordaz G, The US. Department of energy's national hydrogen storage project: progress towards meeting hydrogen-powered vehicle requirements. Catal Today 2007;120:246–56.
[4] Zubizarreta L, Arenillas A, Pis JJ. Carbon materials for H_2 storage. Int J Hydrogen Energy 2009;34:4575–81.
[5] Yürüm Y, Taralp A, NejatVeziroglu T. Storage of hydrogen in nanostructured carbon materials. Int J Hydrogen Energy 2009;34:3784–98.
[6] Zhao W, Fierro V, Zlotea C, Aylon E, Izquierdo MT, Latroche M, et al. Optimization of activated carbons for hydrogen storage. Int J Hydrogen Energy 2011;36:11746–51.
[7] Huang C-C, Chen H-M, Chn C-H. Hydrogen adsorption on modified activated carbon. Int J Hydrogen Energy 2010;35: 2777–80.
[8] Wang Z, Yang RT. Enhanced hydrogen storage on Pt-doped carbon by plasma reduction. J Phys Chem C 2010;114: 5956–63.
[9] Zubizarreta L, Menéndez JA, Pis JJ, Arenillas A. Improving hydrogen storage in Ni-doped carbon nanospheres. Int J Hydrogen Energy 2009;34:300–76.

[10] Saha D, Deng S. Hydrogen adsorption on ordered mesoporous carbons doped with Pd, Pt, Ni and Ru. Langmuir 2009;25:12550–60.
[11] Chen C-H, Huang C-C. Enhancement of hydrogen spillover onto carbon nanotubes with defect feature. Micropor Mesopor Mat 2008;109:549–59.
[12] Wang L, Yang RT. New sorbents for hydrogen storage by hydrogen spillover- a review. Energy Environ Sci 2008;1: 268–79.
[13] Zacharia R, Rather S-U, Hwang SW, Nahm KS. Spillover of physisorbed hydrogen from sputter-deposited arrays of platinum nanoparticles on multi-walled carbon nanotubes. Chem Phys Lett 2007;434:286–91.
[14] Hsieh C-T, Chou Y-W, Lin J-Y. Fabrication and electrochemical activity of Ni-attached carbon nanotube electrodes for hydrogen storage in alkali electrolyte. Int J Hydrogen Energy 2007;32:3457–64.
[15] Jin GP, Ding YF, Zhen PP. Electrodeposition of nickel nanoparticles on functional MWCNT surfaces for ethanol oxidation. J Power Sources 2007;166:80–6.
[16] Bittencourt C, Felte A, Ghijsen J, PireauxJJ Drube W, Erni R, Tendeloo GV. Decorating carbon nanotubes with nickel nanoparticles. Chem Phys Lett 2007;436:368–72.
[17] Wu Z, Ge S, Zhang M, Li W, Tao K. Synthesis of nickel nanoparticles supported on metal oxides using electroless plating: controlling the dispersion and size of nickel nanoparticles. J Colloid Interf Sci 2009;330:359–66.
[18] Chen C-Y, Lin K-Y, Tsai W-T, Chang J-K. Tseng C-M.Electroless deposition of Ni nanoparticles on carbon nanotubes with the aid of supercritical CO_2 fluid and a synergistic hydrogen storage property of the composite. Int J Hydrogen Energy 2010;35:5490–7.
[19] Kim B-J, Lee Y-S, Park S-J. A study on the hydrogen storage capacity of Ni-plated porous carbon nanofibers. Int J Hydrogen Energy 2008;33:4112–5.
[20] Wang Yi, Wang Kean, Guan Cong, He Ziming, Lu Zhisong, Chen Tao, et al. Surface functionalization-enhanced spillover effect on hydrogen storage of Ni-B nanoalloy-doped activated carbon. Int J Hydrogen Energy 2011;36:13663–8.
[21] Mallory GO, Hajdu JB. Electroless plating Fundamentals and applications, Orlando. Fl: American Electroplaters and Surface Finishers Society INC (AESF); 1991.
[22] Lin Kuan-Yu, Tsai Wen-Ta, Yang Tsong-Jen. Effect of Ni nanoparticle distribution on hydrogen uptake in carbon nanotubes. J Power Source 2011;196:3389–94.
[23] Haag S, Burgard M, Ernst B. Pure nickel coating on a mesoporous alumina membrane: preparation by electroless plating and characterization. Surf Coat Tech 2006; 201:2166–73.
[24] Brunauer S, Emmett PH, Teller E. Adsorption of gases in multimolecular layers. J Am Chem Soc 1938;60:309–19.
[25] Sing KSW, Everett DH, Haul RAW, Moscou L, Pierotti RA, Rouqerol J, et al. Reporting physisorption data for gas/solid systems with special reference to the determination of surface area and porosity. Pure Appl Chem 1985;57:603–19.
[26] Marsh H, Rodríguez-Reinoso F. Activated carbon. Oxford, USA: Elsevier; 2006.
[27] Cheng YS, Yeung KL. Effects of electroless plating chemistry on the synthesis of palladium membranes. J Membr Sci 2001; 182:195–203.
[28] DOE criterion. http://www.energy.gov/energysources/hydrogen.htm.
[29] Driessen A, Sänger P, Hemmes H, Griessen R. Metal hydride formation at pressures up to 1MPa. J Phys Condens Matter 1990;2:9797–814.
[30] Wang L, Yan FH, Yang RT. Effect of surface oxygen groups in carbons on hydrogen storage by spillover. Ind Eng Chem Res 2009;48:2920–6.
[31] Wang L, Yang RT. Hydrogen storage properties of carbons doped with ruthenium, platinum and nickel nanoparticles. J Phys Chem C 2008;112:12486–94.
[32] Zielinski M, Wojcieszak R, Monteverdi S, Mercy M, Bettahar MM. Hydrogen storage in nickel catalysts supported on activated carbon. Int J Hydrogen Energy 2007;32:1024–32.
[33] Lin Kuan-Yu, Tsai Wen-Ta, Chang Jeng-Kuei. Decorating carbon nanotubes with Ni particles using an electroless deposition technique for hydrogen storage applications. Int J Hydrogen Energy 2010;35:7555–62.
[34] Kim Byung-Joo, Park Soo-Jin. Optimization of the pore structure of nickel/graphite hybrid materials for hydrogen storage. Int J Hydrogen Energy 2011;36:648–53.
[35] Moradi SE, Amirmahmoodi S, Baniamerian MJ. Hydrogen adsorption in metal-doped highly ordered mesoporous carbon molecular sieve. J Alloy Comp 2010;498:168–71.